

VC dimension of Graph Neural Networks with Pfaffian activation functions

Giuseppe Alessio D’Inverno, Monica Bianchini, Franco Scarselli

Department of Information Engineering and Mathematics
University of Siena
Via Roma 56, I-53100, Siena, Italy

Abstract

Graph Neural Networks (GNNs) have emerged in recent years as a powerful tool to learn tasks across a wide range of graph domains in a data–driven fashion. Based on a message passing mechanism, GNNs have gained increasing popularity due to their intuitive formulation, closely linked to the Weisfeiler–Lehman (WL) test for graph isomorphism, to which they were demonstrated to be equivalent[1, 2]. From a theoretical point of view, GNNs have been shown to be universal approximators, and their generalization capability — related to the Vapnik Chervonekis (VC) dimension [3] — has recently been investigated for GNNs with piecewise polynomial activation functions [4]. The aim of our work is to extend this analysis on the VC dimension of GNNs to other commonly used activation functions, such as the sigmoid and hyperbolic tangent, using the framework of Pfaffian function theory. Bounds are provided with respect to the architecture parameters (depth, number of neurons, input size) as well as with respect to the number of colors resulting from the 1–WL test applied on the graph domain. The theoretical analysis is supported by a preliminary experimental study.

1 Introduction

Since Deep Learning (DL) has become a fundamental tool in approaching real–life applications [5, 6, 7, 8], the urgency of investigating its theoretical properties has become more evident. Neural networks were then progressively studied analyzing, for example, their expressive power in terms of approximating classes of functions [9, 10, 11, 12] or showing their limitations

in the imitation of neurocognitive tasks [13, 14, 15]. The *generalization capability* of a learning model, intended as the capacity of correctly performing a specific task on unseen data, has always been a core aspect to evaluate the effectiveness of proposed architectures [16, 17]. Several metrics and/or methods have been proposed over the years to evaluate such capability [18, 19]. Among them, the *Vapnik Chervonenkis (VC) dimension* [20] is a metric that measures the capacity of a learning model to *shatter* a set of data points, which means that it can always realize a perfect classifier for any binary labeling of the input data. Intuitively, the greater the VC dimension of the learning model, the more it will fit the data on which it has been trained. However, as it has been shown in [21], a large VC dimension leads to poor generalization, i.e. to a large difference between the error evaluated on the training and on the test set. Therefore, it is important to establish the VC dimension of a model, especially with respect to its hyperparameters, in order to make it capable of generalizing on unseen data.

Graph Neural Networks (GNNs) [22, 23] are machine learning architectures capable of processing graphs that represent patterns (or part of patterns) along with their relationships. GNNs are among the most used deep learning models nowadays, given the impressive performance they have shown in tasks related to structured data [24]. A great effort has been dedicated to assess their expressive power, mainly related to the study of the so-called Weisfeiler–Lehman (WL) test [25] and its variants [1, 26, 27]. Indeed, the standard WL algorithm, which checks whether two graphs are isomorphic by iteratively assigning colors to their nodes, has been proved to be equivalent to GNNs in terms of the capability of distinguishing graphs [2]. However, little is known about the generalization capabilities of GNNs. In [3], bounds for the VC dimension have been provided for the original GNN model, namely the first model being introduced. Very recently [4], bounds have been found also for a large class of modern GNNs with piecewise polynomial activation functions. Nevertheless, message passing GNNs with other common activation functions, such as hyperbolic tangent, sigmoid and arctangent, still lack characterization in terms of VC dimension.

This work aims to fill this gap, providing new bounds for modern message passing GNNs with Pfaffian activation functions. *Pfaffian functions* are a large class of differentiable maps, which includes the above mentioned common activation functions, i.e, `tanh`, `logsig`, `atan`, and, more generally, most of the function used in Engineering having continuous derivatives up to any order. Our main contributions are listed below.

- We provide upper bounds for message passing GNNs with Pfaffian

activation functions with respect to the main hyperparameters, such as the feature dimension, the hidden feature size, the number of message passing layers implemented, and the total number of nodes in the entire training domain. To address this issue, we exploit theoretical results in the literature that link the theory of Pfaffian function with the characterization of the VC dimension of GNNs via topological analysis.

- We also study the trend of the VC dimension w.r.t. the colors in the dataset obtained by running the WL test. Theoretical results suggest that the number of colors have an important effect on the GNN generalization capability. On the one hand, a large total number of colors in the training set improves generalization, since it increases the examples available for learning; on the other hand, a large number of colors in each graph raises the VC dimension and therefore increases the empirical risk value.
- Our theoretical findings are assessed by a preliminary experimental study; specifically, we evaluate the gap between the predictive performance on the training and test data.

The manuscript is organized as follows. In Section 2, we offer an overview of work related to the addressed topic. In Section 3, we introduce the main concepts and the notation used throughout the manuscript. In Section 4, we state and discuss our main theoretical results. The preliminary experiments aimed at validating our theoretical results are described in Section 5. Finally, in Section 6, we draw some conclusions, also providing a brief discussion of open problems and future research directions.

2 Related Work

In this section we collect the main contributions present in the literature relating to the generalization ability of GNNs, the calculation of the VC dimension and the theory of Pfaffian functions.

Generalization bounds for GNNs — Several approaches have been exploited to give some insights on the generalization capabilities of GNNs. In [28], new bounds are provided on the *Rademacher complexity* in binary classification tasks; the study is carried out by focusing on the computation trees of the nodes, which are tightly linked to the 1-WL test [29] [30]. Similarly, in [31], generalization bounds for Graph Convolutional Networks (GCNs) are derived, based on the Trasductive Rademacher Complexity,

which differs from the standard Rademacher Complexity by taking into account unobserved instances. In [32], the stability, and consequently the generalization capabilities of GCNs, are proved to be dependent on the largest eigenvalue of the convolutional filter; therefore, to ensure a better generalization, such eigenvalue should be independent of the graph size. Under the lens of the PAC-learnability framework, the generalization bounds reported in [28] have been improved in [33], showing a tighter dependency on the maximum node degree and the spectral norm of the weights. This result aligns with the findings in [32]. In [34], sharper bounds on the GNN stability to noise are provided by investigating the correlation between attention and generalization. Specifically, GCNs and Graph Isomorphism Networks (GINs) are considered. The results show a link between the trace of the Hessian of the weight matrices and the stability of GNNs. A correlation between attention and generalization in GCNs and GINs is empirically investigated also in [35].

VC dimension — Since it was first introduced in [20], the VC dimension has become a widespread metric to assess the generalization capabilities of neural networks. In [36], the VC dimension is proven to be tightly related to how the test error correlates, in probability, with the training error. Bounds on the VC dimension have been evaluated for many baseline architectures, such as Multi Layer Perceptrons (MLPs) [37] [38], Recurrent Neural Networks (RNNs) [39] and Recursive Neural Networks [3]. In [3], bounds on the VC dimension of the earliest GNN model with Pfaffian activation function are provided as well, while, in [31], GCNs with linear and ReLU activation functions are considered. Our contribution extends such results to generic GNNs described by Eq. (1) and is particularly related to the work in [4], where bounds for the VC dimension of modern GNNs are studied, when the activation function is a piecewise linear polynomial function. Bounds are derived also in terms of the number of colors computed by the 1-WL test on the graph domain. However, aside from [3], all the aforementioned works focus solely on specific GNN models with piecewise polynomials activation functions, not considering common activation functions as arctangent, hyperbolic tangent or sigmoid.

Pfaffian functions — Pfaffian functions have been first introduced in [40] to extend Bezout’s classic theorem, which states that the number of complex solutions of a set of polynomial equations can be estimated based on their degree. The theory of Pfaffian functions has been exploited initially

in [41] to characterize the bounds of the VC dimension of neural networks. Similarly, in [3], the same approach is used to provide the aforementioned bounds. Pfaffian functions have also proven useful for providing insights into the topological complexity of neural networks and the impact of their depth [42].

3 Notation and basic concepts

In this section we introduce the notation used throughout the paper and the main basic concepts necessary to understand its content.

Graphs — An *unattributed graph* G can be defined as a pair (V, E) , where V is the (finite) set of *nodes* and $E \subseteq V \times V$ is the set of *edges* between nodes. A graph can be defined by its *adjacency matrix* \mathbf{A} , where $A_{ij} = 1$ if $e_{ij} = (i, j) \in E$, otherwise $A_{ij} = 0$. The *neighborhood* of a node v is represented by $\text{ne}(v) = \{u \in V | (u, v) \in E\}$. A graph G is said to be *undirected* if it is assumed that $(v, u) = (u, v)$ (and therefore its adjacency matrix is symmetric), *directed* otherwise. A graph is said to be *node-attributed* or *labeled* if there exists a map $\alpha : V \rightarrow \mathbb{R}^q$ that assigns to every $v \in V$ a *node attribute* (or *label*) $\alpha(v) \in \mathbb{R}^q$. In this case, the graph can be defined as a triple (V, E, α) .

The 1–WL test — The *1st order Weisfeiler–Lehman test* (briefly, the *1–WL test*) is a test for graph isomorphism, based on the so-called *color refinement* procedure. Given two graphs $G_1 = (V_1, E_1)$ and $G_2 = (V_2, E_2)$, in a finite graph domain \mathcal{G} , we perform the following steps.

- At initialisation, we assign a color $c^{(0)}(v)$ to each node $v \in V_1 \cup V_2$. Formally, in the case of attributed graphs, we can define the color initialisation as

$$c^{(0)}(v) = \text{HASH}_0(\alpha(v)),$$

where $\text{HASH}_0 : \mathbb{R}^q \rightarrow \Sigma$ is a function that codes bijectively node attributes to colors. In case of unattributed graphs, the initialisation is uniform, and each node v gets the same color $c^{(0)}(v)$.

- For $t > 0$, we update the color of each node in parallel on each graph by the following updating scheme

$$c_v^{(t)} = \text{HASH}(c_v^{(t-1)}, \{c_u^{(t-1)} | u \in \text{ne}[v]\}), \quad \forall v \in V_1 \cup V_2,$$

where $\text{HASH} : \Sigma \times \Sigma^* \rightarrow \Sigma$ is a function mapping bijectively a pair (color, color multiset) to a single color.

To test whether the two graphs G_1 and G_2 are isomorphic or not, the set of colors of the nodes of G_1 and G_2 are compared step by step; if there exist an iteration t such that the colors are different, namely $c_{G_1}^{(t)} := \{\{c^{(t)}(v) \mid v \in V_1\}\}$ is different from $c_{G_2}^{(t)}$, the graphs are declared as non-isomorphic. When no difference is detected, the procedure halts as soon as the node partition defined by the colors becomes stable. It has been proven [43] that $|V| - 1$ iterations are sufficient, and sometimes necessary, to complete the procedure. Moreover, the color refinement procedure can be used also to test whether two nodes are isomorphic or not. Intuitively, two nodes are isomorphic if their neighborhoods (of any order) are equal; such an isomorphism can be tested by comparing the node colors at any step of the 1-WL test. In [29], it has been proven that for node isomorphism up to $2 \max(|V_1|, |V_2|) - 1$ refinement steps may be required.

We would like to mention two important results that demonstrate the equivalence between GNNs and the 1-WL test in terms of their expressive power. The first result was established in [2] and characterizes the equivalence of GNNs and the 1-WL test on a graph-level task. This equivalence is based on GNNs with generic message passing layers that satisfy certain conditions. Another characterization is due to [1] and states the equivalence on a node coloring level, referring to the particular model defined by Eq. (2).

Graph Neural Networks (GNNs) — Graph Neural Networks are a class of machine learning models suitable for processing structured data in the form of graphs. At a high level, we can formalize a GNN as a function $\mathbf{g} : \mathcal{G} \rightarrow \mathbb{R}^r$, where \mathcal{G} is a set of node-attributed graphs and r is the dimension of the output, which depends on the type of task to be carried out; in our setting, we will assume that $r = 1$. Intuitively, a GNN learns how to represent the nodes of a graph by vectorial representations, called *hidden features*, giving an encoding of the information stored in the graph. The hidden feature \mathbf{h}_v of a node v is, at the beginning set equal to node attributes, i.e., $\mathbf{h}_v^{(0)} = \boldsymbol{\alpha}(v)$. Then, the features are updated according to the following schema

$$\mathbf{h}_v^{(t+1)} = \text{COMBINE}^{(t+1)}(\mathbf{h}_v^{(t)}, \text{AGGREGATE}^{(t+1)}(\{\mathbf{h}_u^{(t)} \mid u \in \text{ne}(v)\})), \quad (1)$$

for all $v \in V$ and $t = 0, \dots, L - 1$, where $\mathbf{h}_v^{(t)}$ is the hidden feature of node v at time t , L is the number of layers of the GNN and $\{\cdot\}$ denotes a multiset. Here $\{\text{COMBINE}^{(t)}\}_{t=1, \dots, L}$ and $\{\text{AGGREGATE}^{(t)}\}_{t=1, \dots, L}$ are functions that can be

defined by learning from examples. Popular GNN models like GraphSAGE [44], GCNs [45], and Graph Isomorphism Networks [2] are based on this updating scheme. The output o is produced by a **READOUT** function, which, in graph-focused tasks, takes in input the features of all the nodes, i.e. $o = \text{READOUT}(\{\mathbf{h}_u^{(L)} | u \in V\})$, while, in node-focused tasks, is calculated on each node, i.e., $o_v = \text{READOUT}(\mathbf{h}_v^{(L)})$, $\forall v \in V$.

For simplicity, in the following we will assume that **COMBINE**⁽¹⁾ has $p_{\text{comb}}^{(1)}$ parameters and for every $t = 2, \dots, L$ the number of parameters of **COMBINE**^(t) is the same, and we denote it as p_{comb} . The same holds for **AGGREGATE**^(t) and **READOUT**, with the number of parameters denoted respectively as p_{agg} and p_{read} . Thus, the total number of parameters in a GNN defined as in Eq. (1) is $\bar{p} = p_{\text{comb}}^{(1)} + p_{\text{agg}}^{(1)} + (L - 1)(p_{\text{comb}} + p_{\text{agg}}) + p_{\text{read}}$.

For our analysis, following [1], we also consider a simpler computational framework, which has been proven to match the expressive power of the Weisfeiler–Lehman test [1], and is general enough to be similar to many GNN models. In such a framework, the hidden feature $\mathbf{h}_v^{(t+1)} \in \mathbb{R}^d$ at the message passing iteration $t + 1$ is defined as

$$\mathbf{h}_v^{(t+1)} = \sigma(\mathbf{W}_{\text{comb}}^{(t+1)} \mathbf{h}_v^{(t)} + \mathbf{W}_{\text{agg}}^{(t+1)} \mathbf{h}_{\text{ne}(v)}^{(t)} + \mathbf{b}^{(t+1)}), \quad (2)$$

where $\mathbf{h}_{\text{ne}(v)}^{(t)} = \text{POOL}(\{\mathbf{h}_u^{(t)} | u \in \text{ne}(v)\})$, $\sigma : \mathbb{R}^d \rightarrow \mathbb{R}^d$ is an element-wise activation function, and **POOL** is the aggregating operator on the features of neighboring nodes,

$$\text{POOL}(\{\mathbf{h}_u^{(t)} | u \in \text{ne}(v)\}) = \sum_{u \in \text{ne}(v)} \mathbf{h}_u^{(t)}.$$

With respect to Eq. (1), we have that $\text{AGGREGATE}^{(t)}(\cdot) = \text{POOL}(\cdot) \forall t = 1, \dots, L$, while $\text{COMBINE}^{(t+1)}(\mathbf{h}_v, \mathbf{h}_{\text{ne}(v)}) = \sigma(\mathbf{W}_{\text{comb}}^{(t+1)} \mathbf{h}_v + \mathbf{W}_{\text{agg}}^{(t+1)} \mathbf{h}_{\text{ne}(v)} + \mathbf{b}^{(t+1)})$. In this case, the **READOUT** function for graph classification tasks can be defined as

$$\text{READOUT}(\{\mathbf{h}_v^{(L)} | v \in V\}) := f\left(\sum_{v \in V} \mathbf{w} \mathbf{h}_v^{(L)} + b\right). \quad (3)$$

For each node, the hidden state is initialized as $\mathbf{h}_v^{(0)} = \boldsymbol{\alpha}(v) \in \mathbb{R}^q$. The learnable parameters of the GNN can be summarized as

$$\boldsymbol{\Theta} := (\mathbf{W}_{\text{comb}}^{(1)}, \mathbf{W}_{\text{agg}}^{(1)}, \mathbf{b}^{(1)}, \mathbf{W}_{\text{comb}}^{(2)}, \mathbf{W}_{\text{agg}}^{(2)}, \mathbf{b}^{(2)}, \dots, \mathbf{W}_{\text{comb}}^{(L)}, \mathbf{W}_{\text{agg}}^{(L)}, \mathbf{b}^{(L)}, \mathbf{w}, b),$$

with $\mathbf{W}_{\text{comb}}^{(1)}, \mathbf{W}_{\text{agg}}^{(1)} \in \mathbb{R}^{d \times q}$, $\mathbf{W}_{\text{comb}}^{(t)}, \mathbf{W}_{\text{agg}}^{(t)} \in \mathbb{R}^{d \times d}$, for $t = 2, \dots, L$, $\mathbf{b}^{(t)} \in \mathbb{R}^{d \times 1}$, for $t = 2, \dots, L$, $\mathbf{w} \in \mathbb{R}^{1 \times d}$, and $b \in \mathbb{R}$.

VC dimension — The VC dimension is a measure of complexity of a set of hypotheses, which can be used to bound the empirical error of machine learning models. Formally, a binary classifier \mathcal{L} with parameters $\boldsymbol{\theta}$ is said to *shatter* a set of patterns $\{\mathbf{x}_1, \dots, \mathbf{x}_n\} \subseteq \mathbb{R}^q$ if, for any binary labeling of the examples $\{y_i\}_{i=1, \dots, n}$, $y_i \in \{0, 1\}$, there exists $\boldsymbol{\theta}$ s.t. the model \mathcal{L} correctly classifies all the patterns, i.e. $\sum_{i=0}^n |\mathcal{L}(\boldsymbol{\theta}, \mathbf{x}_i) - y_i| = 0$. The *VC dimension* of the model \mathcal{L} is the dimension of the largest set that \mathcal{L} can shatter.

The VC dimension is linked with the generalization capability of machine learning models. Actually, given a training and a test set for the classifier \mathcal{L} , whose patterns are i.i.d. samples extracted from the same distribution, the VC dimension allows to compute a bound, in probability, for the difference between the training and test error [46]:

$$\Pr\left(E_{\text{test}} \leq E_{\text{training}} + \sqrt{\frac{1}{N} \left[\text{VCdim} \left(\log \left(\frac{2N}{\text{VCdim}} \right) + 1 \right) - \log \left(\frac{\eta}{4} \right) \right]}\right) = 1 - \eta$$

for any $\eta > 0$, where E_{test} is the test error, E_{training} is the training error, N is the size of the training dataset and VCdim is the VC dimension of \mathcal{L} .

Pfaffian Functions — A Pfaffian chain of order $\ell \geq 0$ and degree $\alpha \geq 1$, in an open domain $U \subseteq \mathbb{R}^n$, is a sequence of analytic functions f_1, f_2, \dots, f_ℓ over U , satisfying the differential equations

$$df_j(\mathbf{x}) = \sum_{1 \leq i \leq n} g_{ij}(\mathbf{x}, f_1(\mathbf{x}), \dots, f_j(\mathbf{x})) dx_i, \quad 1 \leq j \leq \ell.$$

Here, $g_{ij}(\mathbf{x}, y_1, \dots, y_j)$ are polynomials in $\mathbf{x} \in U$ and $y_1, \dots, y_j \in \mathbb{R}$ of degree not exceeding α . A function $f(\mathbf{x}) = P(\mathbf{x}, f_1(\mathbf{x}), \dots, f_\ell(\mathbf{x}))$, where $P(\mathbf{x}, y_1, \dots, y_\ell)$ is a polynomial of degree not exceeding β , is called a *Pfaffian function of format* (α, β, ℓ) .

Pfaffian maps are a large class of functions that include most of the functions with continuous derivatives used in practical applications [40]. In particular, the arctangent `atan`, the logistic sigmoid `logsig` and the hyperbolic tangent `tanh` are Pfaffian functions, with format `format(atan) = (3, 1, 2)`, `format(logsig) = (2, 1, 1)`, and `format(tanh) = (2, 1, 1)`, respectively.

4 Theoretical results

In this section we report the main results on the VC dimension of GNNs with Pfaffian activation functions. The proofs can be found in Appendix A.

4.1 Bounds based on the network hyperparameters

Our main result provides a bound on the VC dimension of GNNs in which $\text{COMBINE}^{(t)}$, $\text{AGGREGATE}^{(t)}$ and READOUT are Pfaffian functions. More precisely, we consider a slightly more general version of the GNN model in Eq. (1), where the updating scheme is

$$\mathbf{h}_v^{(t+1)} = \text{COMBINE}^{(t+1)}(\mathbf{h}_v^{(t)}, \text{AGGREGATE}^{(t+1)}(\{\mathbf{h}_u^{(t)} | u \in V\}, A_v)), \quad (4)$$

and A_v is the v -th column of the connectivity matrix, which represents the neighborhood of v . The advantage of the model in Eq. (4) is that it makes explicit the dependence of $\text{AGGREGATE}^{(t)}$ on the graph connectivity. Actually, here we want to underline what the inputs of $\text{AGGREGATE}^{(t)}$ are to clarify and make formally precise the assumptions that those functions are Pfaffian and have a given format.

Our result provides a bound on the VC dimension w.r.t. the total number \bar{p} of parameters, the number of computation units H , the number of layers L , the feature dimension d , the maximum number N of nodes in a graph, and the attribute dimension q . Here, we assume that GNN computation units include the neurons computing the hidden features of each node and the outputs. Therefore, there is a computation unit for each component of a feature, each layer, each node of the input graph and a further computation unit for the READOUT .

Theorem 1. Let us consider the GNN model described by Eq. (1). If $\text{COMBINE}^{(t)}$, $\text{AGGREGATE}^{(t)}$ and READOUT are Pfaffian functions with format $(\alpha_{\text{comb}}, \beta_{\text{comb}}, \ell_{\text{comb}})$, $(\alpha_{\text{agg}}, \beta_{\text{agg}}, \ell_{\text{agg}})$, $(\alpha_{\text{read}}, \beta_{\text{read}}, \ell_{\text{read}})$, respectively, then the VC dimension satisfies

$$\text{VCdim}(\text{GNN}) \leq 2 \log B + \bar{p}(16 + 2 \log \bar{s}) \quad (5)$$

where $B \leq 2^{\frac{\bar{\ell}(\bar{\ell}-1)}{2}+1}(\bar{\alpha}+2\bar{\beta}-1)^{\bar{p}-1}((2\bar{p}-1)(\bar{\alpha}+\bar{\beta})-2\bar{p}+2)^{\bar{\ell}}$, $\bar{\alpha} = \max\{\alpha_{\text{agg}} + \beta_{\text{agg}} - 1 + \alpha_{\text{comb}}\beta_{\text{agg}}, \alpha_{\text{read}}\}$, $\bar{\beta} = \max\{\beta_{\text{comb}}, \beta_{\text{read}}\}$, $\bar{p} = p_{\text{comb}^{(0)}} + p_{\text{agg}^{(0)}} + (L-1)(p_{\text{comb}} + p_{\text{agg}}) + p_{\text{read}}$, $\bar{\ell} = \bar{p}H$, $H = LNd(\ell_{\text{comb}} + \ell_{\text{agg}}) + \ell_{\text{read}}$ and $\bar{s} = LNd + Nq + 1$ hold. By substituting the definitions in Eq. (5), we obtain

$$\begin{aligned} \text{VCdim}(\text{GNN}) &\leq \bar{p}^2(LNd(\ell_{\text{comb}} + \ell_{\text{agg}}) + \ell_{\text{read}})^2 \\ &\quad + 2\bar{p}\log(3\gamma) \\ &\quad + 2\bar{p}\log((4\gamma-2)\bar{p})+2-2\gamma \\ &\quad + \bar{p}(16 + 2 \log(LNd + Nq + 1)) \end{aligned} \quad (6)$$

where $\bar{\alpha}, \bar{\beta} \leq \gamma$ for a constant $\gamma \in \mathbb{R}$.

By inspecting the bound, we observe that the dominant term is $\bar{p}^2 H^2 = \bar{p}^2 (LNd(\ell_{\text{comb}} + \ell_{\text{agg}}) + \ell_{\text{read}})^2$. Thus, Theorem 1 suggests that the VC dimension is $O(\bar{p}^2 L^2 N^2 d^2)$, w.r.t. the number of parameters \bar{p} of the GNN, the number of layers L , the number N of graph nodes, and the feature dimension d . Notice that those hyperparameters are related by constraints, which should be considered in order to understand how the VC dimension depends on each of them. Therefore, the VC dimension is at most $O(p^4)$ since, as the number p of parameters grows, the number of layers L and/or the feature dimension d also increases.

Interestingly, such a result is similar to those already obtained for feed-forward and recurrent neural networks with Pfaffian activation functions. Table 1 compares our result with those available in the literature, highlighting that, even if GNNs have a more complex structure, the growth rate of the VC dimension, depending on the hyperparameters, is the same as the simpler models.

The following theorem provides more details and clarifies how the VC dimension depends on each hyperparameter.

Theorem 2. Let $\text{COMBINE}^{(t)}$, $\text{AGGREGATE}^{(t)}$ and READOUT be the Pfaffian functions defined in Theorem 1. If $p_{\text{comb}}, p_{\text{aggr}}, p_{\text{read}} \in \mathcal{O}(d)$, then the VC dimension of a GNN defined as in Eq. (1), w.r.t. \bar{p}, N, L, d, q satisfies

$$\begin{aligned}\text{VCdim}(\text{GNN}) &\leq \mathcal{O}(\bar{p}^4) \\ \text{VCdim}(\text{GNN}) &\leq \mathcal{O}(N^2) \\ \text{VCdim}(\text{GNN}) &\leq \mathcal{O}(L^4) \\ \text{VCdim}(\text{GNN}) &\leq \mathcal{O}(d^6) \\ \text{VCdim}(\text{GNN}) &\leq \mathcal{O}(q^2)\end{aligned}$$

□

The proof of Theorem 1 adopts the same reasoning used in [41] to derive a bound on the VC dimension of feedforward neural networks with Pfaffian activation functions, and used in [3] to provide a bound for the first GNN model. Intuitively, the proof is based on the following steps: it is shown that the computation of the GNNs on graphs can be represented by a set of equations defined by Pfaffian functions with format $(\bar{\alpha}, \bar{\beta}, \bar{\ell})$, where $\bar{\alpha}, \bar{\beta}, \bar{\ell}$ are those defined in the theorem; then, the bound is obtained exploiting a result in [41] that associates the VC dimension to the number of connected components in the inverse image of a system of Pfaffian equations. Finally, a result in [53] allows to estimate the required number of connected

Activation function	Bound	References
Modern GNNs		
Piecewise polynomial	$O(p \log(\mathcal{C}p) + p \log(N))$	[4]
\tanh , logsig or atan	$O(p^4 N^2)$	this work
\tanh , logsig or atan	$O(p^4 \mathcal{C}^2)$	this work
Original GNNs [22]		
Polynomial	$O(p \log(N))$	[3]
Piecewise polynomial	$O(p^2 N \log(N))$	[3]
\tanh , logsig or atan	$O(p^4 N^2)$	[3]
Positional RecNNs		
Polynomial	$O(pN)$	[47]
logsig	$O(p^4 N^2)$	[47]
Recurrent Neural Networks		
Polynomial	$O(pN)$	[48]
Piecewise polynomial	$O(p^2 N)$	[48]
\tanh or logsig	$O(p^4 N^2)$	[48]
Multilayer Networks		
Binary	$O(p \log p)$	[49, 50, 51]
Polynomial	$O(p \log p)$	[52]
Piecewise polynomial	$O(p^2)$	[52, 48]
\tanh , logsig or atan	$O(p^4)$	[41]

Table 1: Upper bounds on the VC dimension of common architectures, where p is the number of network parameters, N the number of nodes in the input graph or sequence, and \mathcal{C} the maximum number of colors per graph.

components. Note that our bound and other bounds obtained for networks with Pfaffian activation functions are larger than those for networks with simpler activations. As explained in [41] [3], such a difference is likely due to the current limitations of mathematics in this field, which makes tight bounds more difficult to achieve with Pfaffian functions.

We now specifically derive bounds for the VC dimension for the architecture described by Eqs. (2)–(3).

Theorem 3. Let us consider the GNN model described by Eqs. (2)–(3). If σ is a Pfaffian function in \mathbf{x} with format $(\alpha_\sigma, \beta_\sigma, \ell_\sigma)$, then the VC dimension satisfies

$$\text{VCdim}(\text{GNN}) \leq 2 \log B + \bar{p}(16 + 2 \log \bar{s}),$$

where $B \leq 2^{\frac{\bar{\ell}(\bar{\ell}-1)}{2}+1}(\bar{\alpha} + 2\bar{\beta} - 1)^{\bar{p}-1}((2\bar{p}-1)(\bar{\alpha} + \bar{\beta}) - 2\bar{p} + 2)^{\bar{\ell}}$, $\bar{\alpha} = 2 + 3\alpha_\sigma$, $\bar{\beta} = \beta_\sigma$, $\bar{\ell} = \bar{p}H\ell_\sigma$, and $\bar{s} = LNd + Nq + 1$ hold.

In particular, if σ is the logistic sigmoid activation function, we have

$$\text{VCdim}(\text{GNN}) \leq \bar{p}^2 H^2 + 2\bar{p} \log(9) + 2\bar{p}H \log(16\bar{p}) + \bar{p}(16 + 2 \log(\bar{s})).$$

□

The proof of Theorem 3 can be found in Appendix A.

Interestingly, the bounds on the VC dimension that can be derived from Theorem 3, w.r.t the hyperparameters, turn out to be the same derived in Theorem 2. Thus, even if the considered model is simpler, those bounds do not change.

4.2 Bounds based on the number of the 1–WL colors

The developed theory is also easily applied to the case when nodes are grouped according to their colors defined by the Weisfeiler–Lehman algorithm. Intuitively, since GNNs produce the same features on group of nodes with the same color, the computation can be simplified by considering each group as a single entity. As consequence, the bounds on VC dimension can be tightened by using colors in place of nodes. Formally, for a given graph G , let $C_1(G) = \sum_{i=1}^T C^t(G)$ be the number of colors generated by the 1–WL test, where $C^t(G)$ is the number of colors at step $t > 0$. Moreover, let us assume that $C^t(G)$ is bounded, namely there exists C_1 such that $C_1(G) \leq C_1$ for all the graphs G in the domain \mathcal{G} . The following theorem provides a bound on the VC dimension w.r.t. the number of colors produced by the 1–WL test.

Theorem 4. Let us consider the GNN model described by Eqs. (2)–(3) using the logistic sigmoid `logsig` as the activation function. Assume a subset $\mathcal{S} \subseteq \mathcal{G}$. The VC dimension of the GNN satisfies

$$\begin{aligned}\text{VCdim}(\text{GNN}(C_1)) &\leq \mathcal{O}(C_1^2) \\ \text{VCdim}(\text{GNN}(C_0)) &\leq \mathcal{O}(\log(C_0))\end{aligned}$$

□

The theorem suggests that the VC dimension depends quadratically on the total number of node colors and logarithmically on the initial number of colors. Actually, a GNN processes all the nodes of a graph at the same time and the GNN architecture is similar to a feedforward network where some computation units are replicated at each node. Thus, the complexity of the GNN grows with the number of nodes and this explains the dependence of the VC dimension on the number of nodes (see Theorem 2). On the other hand, nodes with the same colors cannot be distinguished by the GNN: this means that, in theory, we can use the same computation units for a group of nodes sharing the color. Therefore, to get tighter bounds on the VC dimension, we can consider the number of colors in place of the number of nodes.

Finally, it is worth mentioning that, the presented theorems suggest that GNNs may have a worst generation capability when the domain is composed by graphs with many different colors. This happens because when the number of colors in each graph increases, the VC dimension increases as well. On the other hand, the generalization capability benefits from a large total number of colors in the training set. Actually, generalization depends not only on VC dimension, but, obviously, also on the number of patterns in training set (see Eq. (3)). In GNN graph–focused tasks, graphs play the role of patterns, where we count only the graphs with different colors, as those with the same colors are just copies of the same pattern. A similar reasoning applies to node–focused task, by counting the total number of nodes with different color in training set.

5 Experimental validation

In this section, we present an experimental validation of our theoretical results. We will show how the VC dimension of GNNs, described in Eqs. (2)–(3), changes as the hyperparameters vary, respecting the bounds found in Theorems 2 and 4.

5.1 Experimental setting

We design two experiments to assess the validity, respectively, of Theorems 2 and 4. In both cases, we train a Graph Neural Network, composed by message passing layers, defined as in Eq. (2), where the activation function σ is \arctan or \tanh ; the final READOUT layer is an affine layer with $\mathbf{W}_{\text{out}} \in \mathbb{R}^{1 \times \text{hd}}$, after which a logsig activation function is applied. The model is trained via Adam optimizer with an initial learning rate $\lambda = 10^{-3}$. The hidden feature size is denoted by hd and the number of layers by l .

E1: We measure the evolution of the difference between the training accuracy and the validation accuracy, $\text{diff} = \text{training_acc} - \text{test_acc}$, through the training epochs, over three different datasets taken from the TUDataset repository [54]. In particular, **PROTEINS** [55] is a dataset of proteins represented as graphs which contains both enzymes and non-enzymes; **NCI1** [56] is a dataset of molecules relative to anti-cancer screens where the chemicals are assessed as positive or negative to cell lung cancer; finally, **PTC-MR** [57] is a collection of chemical compounds represented as graphs which report the carcinogenicity for rats. The choice of the datasets has been driven by their binary classification nature. Their statistics are summarized in Table 2. In the experiments, firstly, we fix the hidden feature size to $\text{hd} = 32$ and let the number of layers vary in the range $l \in [2, 3, 4, 5, 6]$, to measure how diff evolves. Subsequently, we fix the number of layers to $l = 3$ and let the hidden feature size vary in the range, $\text{hd} \in [8, 16, 32, 64, 128]$, to perform the same task. We train the model for 500 epochs in each run, with the batch size set to 32.

E2: We measure the evolution of the difference between the training accuracy and the validation accuracy, diff , through the training epochs over the dataset **NCI1**, whose graphs are increasingly ordered according to the ratio $\frac{|V(G)|}{C^t(G)}$ and split in four different groups. The intuition here is that, being the number of graph nodes bounded, splitting the ordered dataset as described above, should provide four datasets in which the total number of colors is progressively increasing. The hidden size is fixed at $\text{hd} = 16$, the number of layers is $l = 4$, the batch size is fixed equal to 32. In Table 3, we report the reference values for each split. We train the model for 2000 epochs (the number of epochs is greater than in the **E1** task because **E2** shows greater instability during training).

Each experiment is statistically evaluated over 10 runs. The overall

Dataset	# Graphs	# Classes	Avg. # Nodes	Avg. # Edges
PROTEINS	1113	2	39.06	72.82
NCI1	4110	2	29.87	32.30
PTC-MR	344	2	14.29	14.69

Table 2: Statistics on the benchmark datasets used for **E1**.

	Split 1	Split 2	Split 3	Split 4
# Nodes	27667	30591	31763	32673
# Colors	26243	26569	24489	16348
$\min_G \frac{\# \text{Nodes}(G)}{\# \text{Colors}(G)}$	1.000	1.105	1.208	1.437
$\max_G \frac{\# \text{Nodes}(G)}{\# \text{Colors}(G)}$	1.105	1.208	1.437	8

Table 3: Summary of the parameters for each split of the ordered **NCI1** dataset in task **E2**.

training is performed on an Intel(R) Core(TM) i7-9800X processor running at 3.80GHz, using 31GB of RAM and a GeForce GTX 1080 Ti GPU unit. The code developed to run the experiments exploits the Python package `PytorchGeometric` and can be found at <https://github.com/AleDinve/vc-dim-gnn>.

5.2 Experimental results

Task E1 — Numerical results for the **NCI1** dataset are reported in Figures 1 and 2, for `arctan` and `tanh` activations, respectively, while results for **PROTEINS** and **PTC_MR** are reported in Appendix B. In particular, in both Figures 1 and 2, the evolution of `diff` is shown as the number of epochs varies, for different values of `hd` keeping fixed $l = 3$ in (a), and for different values of l keeping fixed `hd` = 32 in (c), respectively. Moreover, the evolution of `diff` as the hidden size increases, for varying epochs, is shown in (b), while (d) depicts how `diff` evolves as the number of layers increases.

The behaviour of the evolution of `diff` proves to be consistent with the bounds provided by Theorem 2 with respect to increasing the hidden dimension or the number of layers. Although it is hard to establish a precise function that links the VC dimension to `diff`, given also the complex nature of Pfaffian functions, we can partially rely on Eq. (3) (which is valid for large sample sets) to argue that our bounds are verified by this experimental setting.

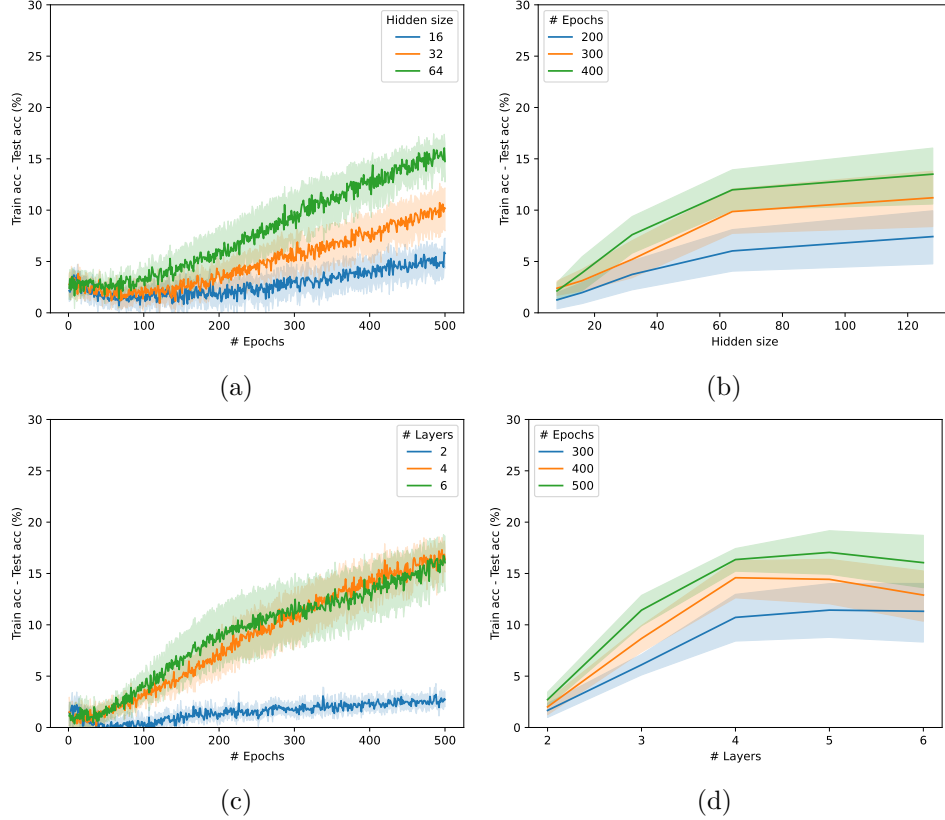


Figure 1: Results on the task **E1** for GNNs with activation function arctan .

Task E2 — Numerical results for this task on the **NCI1** dataset are reported in Figure 3, considering the \tanh activation function. In particular, the evolution of diff is shown in (a) as the number of epochs varies, for different values of $\frac{V(G)}{C^t(G)}$, keeping fixed $l = 4$ and $\text{hd} = 16$; instead, the evolution of diff as the ratio $\frac{V(G)}{C^t(G)}$ increases is depicted in (b), for the number of epochs varying in $\{1000, 1500, 2000\}$.

Similar observations as for the experimental setting **E1** can be drawn here: indeed, the evolution of diff in our experiment is consistent with the bounds presented in Theorem 4, as the ratio between colors and nodes increases.

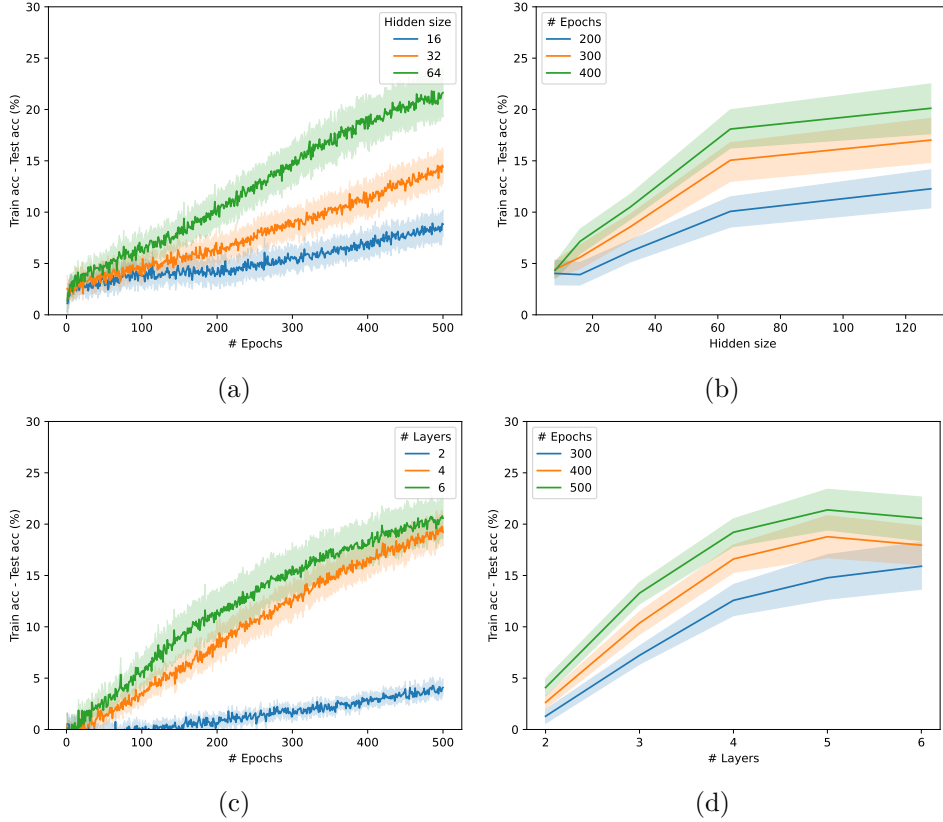


Figure 2: Results on the task **E1** for GNNs with activation function \tanh .

6 Discussion

In this work we derived new bounds for the VC dimension of modern message passing GNNs with Pfaffian activation functions, closing the gap present in the literature with respect to many common used activation functions; furthermore, we propose a preliminary experimental validation to demonstrate the coherence between theory and practice.

Different research perspectives can be envisaged to improve the results obtained: first, our analysis lacks the derivation of *lower bounds*, which could provide a more precise intuition of the degradation of generalization capabilities for GNNs within the chosen architectural framework. In addition, providing a relationship between the VC dimension and the difference between the training and test accuracy would be much more informative; we could establish a quantitative measure with respect to the number of parameters

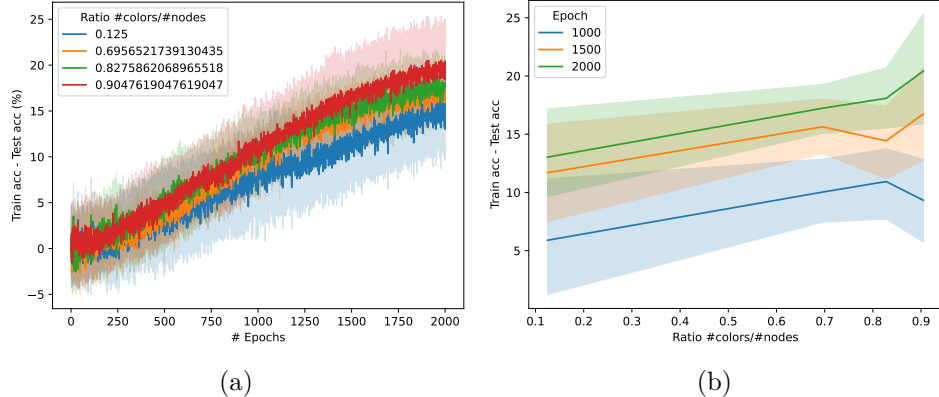


Figure 3: Results on the task **E2** for GNNs with activation function \tanh .

that would allow us to better explain the experimental performance. Finally, the proposed analysis on the VC dimension deserves to be extended to other GNN paradigms, such as Graph Transformers [58] and Graph Diffusion Models [59].

References

- [1] C. Morris, M. Ritzert, M. Fey, W. L. Hamilton, Jan Eric Lenssen, G. Rattan, and M. Grohe. Weisfeiler and leman go neural: Higher-order graph neural networks. In *AAAI Conference on Artificial Intelligence*, pages 4602–4609, 2019.
- [2] K. Xu, W. Hu, J. Leskovec, and S. Jegelka. How powerful are graph neural networks? *International Conference on Machine Learning*, 2019.
- [3] F. Scarselli, A. C. Tsoi, and M. Hagenbuchner. The vapnik-chervonenkis dimension of graph and recursive neural networks. *Neural Networks*, 108:248–259, 2018.
- [4] Christopher Morris, Floris Geerts, Jan Tönshoff, and Martin Grohe. WL meet VC. *Proceedings of the 40th International Conference on Machine Learning*, 2023.
- [5] David Rolnick, Priya L Donti, Lynn H Kaack, Kelly Kochanski, Alexandre Lacoste, Kris Sankaran, Andrew Slavin Ross, Nikola Milojevic-Dupont, Natasha Jaques, Anna Waldman-Brown, et al. Tackling cli-

mate change with machine learning. *ACM Computing Surveys (CSUR)*, 55(2):1–96, 2022.

- [6] Stefania Fresca, Andrea Manzoni, Luca Dedè, and Alfio Quarteroni. Deep learning-based reduced order models in cardiac electrophysiology. *PloS one*, 15(10):e0239416, 2020.
- [7] Remi Lam, Alvaro Sanchez-Gonzalez, Matthew Willson, Peter Wirnsberger, Meire Fortunato, Ferran Alet, Suman Ravuri, Timo Ewalds, Zach Eaton-Rosen, Weihua Hu, et al. Learning skillful medium-range global weather forecasting. *Science*, page eadi2336, 2023.
- [8] John Jumper, Richard Evans, Alexander Pritzel, Tim Green, Michael Figurnov, Olaf Ronneberger, Kathryn Tunyasuvunakool, Russ Bates, Augustin Žídek, Anna Potapenko, et al. Highly accurate protein structure prediction with alphafold. *Nature*, 596(7873):583–589, 2021.
- [9] Kurt Hornik, Maxwell Stinchcombe, and Halbert White. Multilayer feedforward networks are universal approximators. *Neural networks*, 2(5):359–366, 1989.
- [10] Kurt Hornik. Approximation capabilities of multilayer feedforward networks. *Neural networks*, 4(2):251–257, 1991.
- [11] Barbara Hammer. On the approximation capability of recurrent neural networks. *Neurocomputing*, 31(1-4):107–123, 2000.
- [12] Ingrid Daubechies, Ronald DeVore, Simon Foucart, Boris Hanin, and Guergana Petrova. Nonlinear approximation and (deep) relu networks. *Constructive Approximation*, 55(1):127–172, 2022.
- [13] Simone Brugiapaglia, Matthew Liu, and Paul Tupper. Generalizing outside the training set: When can neural networks learn identity effects? *arXiv preprint arXiv:2005.04330*, 2020.
- [14] Simone Brugiapaglia, M Liu, and Paul Tupper. Invariance, encodings, and generalization: learning identity effects with neural networks. *Neural Computation*, 34(8):1756–1789, 2022.
- [15] Giuseppe Alessio D’Inverno, Simone Brugiapaglia, and Mirco Ravanelli. Generalization limits of graph neural networks in identity effects learning. *arXiv preprint arXiv:2307.00134*, 2023.

- [16] Arthur Jacot, Franck Gabriel, and Clément Hongler. Neural tangent kernel: Convergence and generalization in neural networks. *Advances in neural information processing systems*, 31, 2018.
- [17] Behnam Neyshabur, Zhiyuan Li, Srinadh Bhojanapalli, Yann LeCun, and Nathan Srebro. Towards understanding the role of over-parametrization in generalization of neural networks. *arXiv preprint arXiv:1805.12076*, 2018.
- [18] Vladimir Koltchinskii. Rademacher penalties and structural risk minimization. *IEEE Transactions on Information Theory*, 47(5):1902–1914, 2001.
- [19] David Haussler and Manfred Warmuth. The probably approximately correct (PAC) and other learning models. *The Mathematics of Generalization*, pages 17–36, 2018.
- [20] Vladimir N Vapnik and A Ya Chervonenkis. On the uniform convergence of relative frequencies of events to their probabilities. In *Doklady Akademii Nauk USSR*, volume 181, pages 781–787, 1968.
- [21] Vladimir Vapnik. *Estimation of dependences based on empirical data*. Springer Science & Business Media, 2006.
- [22] F. Scarselli, M. Gori, A. C. Tsoi, M. Hagenbuchner, and G. Monfardini. The graph neural network model. *IEEE Transactions on Neural Networks*, 20(1):61–80, 2009.
- [23] Jie Zhou, Ganqu Cui, Shengding Hu, Zhengyan Zhang, Cheng Yang, Zhiyuan Liu, Lifeng Wang, Changcheng Li, and Maosong Sun. Graph neural networks: A review of methods and applications. *AI open*, 1:57–81, 2020.
- [24] Zhiyuan Liu and Jie Zhou. *Introduction to graph neural networks*. Springer Nature, 2022.
- [25] B. Weisfeiler and A. Leman. The reduction of a graph to canonical form and the algebra which appears therein. *Nauchno-Technicheskaya Informatsia*, 2(9):12–16, 1968. English translation by G. Ryabov is available at https://www.iti.zcu.cz/wl2018/pdf/wl_paper_translation.pdf.
- [26] Cristian Bodnar, Fabrizio Frasca, Yuguang Wang, Nina Otter, Guido F Montufar, Pietro Lio, and Michael Bronstein. Weisfeiler and Lehman

Go Topological: Message Passing Simplicial Networks. In *International Conference on Machine Learning*, pages 1026–1037. PMLR, 2021.

[27] Cristian Bodnar, Fabrizio Frasca, Nina Otter, Yuguang Wang, Pietro Lio, Guido F Montufar, and Michael Bronstein. Weisfeiler and lehman go cellular: Cw networks. *Advances in Neural Information Processing Systems*, 34:2625–2640, 2021.

[28] Vikas Garg, Stefanie Jegelka, and Tommi Jaakkola. Generalization and representational limits of graph neural networks. In *International Conference on Machine Learning*, pages 3419–3430. PMLR, 2020.

[29] Andreas Krebs and Oleg Verbitsky. Universal covers, color refinement, and two-variable counting logic: Lower bounds for the depth. In *2015 30th Annual ACM/IEEE Symposium on Logic in Computer Science*, pages 689–700. IEEE, 2015.

[30] Giuseppe Alessio D’Inverno, Monica Bianchini, Maria Lucia Sampoli, and Franco Scarselli. On the approximation capability of GNNs in node classification/regression tasks. *arXiv preprint arXiv:2106.08992*, 2021.

[31] Pascal Esser, Leena Chennuru Vankadara, and Debarghya Ghoshdastidar. Learning theory can (sometimes) explain generalisation in graph neural networks. *Advances in Neural Information Processing Systems*, 34:27043–27056, 2021.

[32] Saurabh Verma and Zhi-Li Zhang. Stability and generalization of graph convolutional neural networks. In *Proceedings of the 25th ACM SIGKDD International Conference on Knowledge Discovery & Data Mining*, pages 1539–1548, 2019.

[33] Renjie Liao, Raquel Urtasun, and Richard Zemel. A PAC-bayesian approach to generalization bounds for Graph Neural Networks. *arXiv preprint arXiv:2012.07690*, 2020.

[34] Haotian Ju, Dongyue Li, Aneesh Sharma, and Hongyang R Zhang. Generalization in Graph Neural Networks: Improved PAC-Bayesian bounds on graph diffusion. In *International Conference on Artificial Intelligence and Statistics*, pages 6314–6341. PMLR, 2023.

[35] Boris Knyazev, Graham W Taylor, and Mohamed Amer. Understanding attention and generalization in graph neural networks. *Advances in neural information processing systems*, 32, 2019.

- [36] Vladimir Vapnik, Esther Levin, and Yann Le Cun. Measuring the vc-dimension of a learning machine. *Neural computation*, 6(5):851–876, 1994.
- [37] Eduardo D Sontag et al. Vc dimension of neural networks. *NATO ASI Series F Computer and Systems Sciences*, 168:69–96, 1998.
- [38] Peter L Bartlett and Wolfgang Maass. Vapnik-chervonenkis dimension of neural nets. *The handbook of brain theory and neural networks*, pages 1188–1192, 2003.
- [39] Pascal Koiran and Eduardo D Sontag. Vapnik-chervonenkis dimension of recurrent neural networks. *Discrete Applied Mathematics*, 86(1):63–79, 1998.
- [40] Askold G Khovanski. *Fewnomials*, volume 88. American Mathematical Soc., 1991.
- [41] Marek Karpinski and Angus Macintyre. Polynomial bounds for VC dimension of sigmoidal and general pfaffian neural networks. *J. Comput. Syst. Sci.*, 54(1):169–176, 1997.
- [42] Monica Bianchini and Franco Scarselli. On the complexity of neural network classifiers: A comparison between shallow and deep architectures. *IEEE transactions on neural networks and learning systems*, 25(8):1553–1565, 2014.
- [43] Sandra Kiefer. The Weisfeiler-Leman algorithm: an exploration of its power. *ACM SIGLOG News*, 7(3):5–27, 2020.
- [44] Will Hamilton, Zhitao Ying, and Jure Leskovec. Inductive representation learning on large graphs. *Advances in Neural Information Processing Systems*, 30, 2017.
- [45] Thomas N Kipf and Max Welling. Semi-supervised classification with graph convolutional networks. *arXiv preprint arXiv:1609.02907*, 2016.
- [46] VN Vapnik and A Ya Chervonenkis. On the uniform convergence of relative frequencies of events to their probabilities. *Theory of Probability & Its Applications*, 16(2):264–280, 1971.
- [47] Barbara Hammer. On the generalization ability of recurrent networks. In *Artificial Neural Networks—ICANN 2001: International Conference Vienna, Austria, August 21–25, 2001 Proceedings 11*, pages 731–736. Springer, 2001.

- [48] Pascal Koiran and Eduardo D Sontag. Neural networks with quadratic vc dimension. *journal of computer and system sciences*, 54(1):190–198, 1997.
- [49] Eric Baum and David Haussler. What size net gives valid generalization? *Advances in neural information processing systems*, 1, 1988.
- [50] Wolfgang Maass. Neural nets with superlinear vc-dimension. *Neural Computation*, 6(5):877–884, 1994.
- [51] Akito Sakurai. On the vc-dimension of depth four threshold circuits and the complexity of boolean-valued functions. *Theoretical computer science*, 137(1):109–127, 1995.
- [52] Paul Goldberg and Mark Jerrum. Bounding the vapnik-chervonenkis dimension of concept classes parameterized by real numbers. In *Proceedings of the sixth annual conference on Computational learning theory*, pages 361–369, 1993.
- [53] Andrei Gabrielov and Nicolai Vorobjov. Complexity of computations with pfaffian and noetherian functions. *Normal forms, bifurcations and finiteness problems in differential equations*, 137:211–250, 2004.
- [54] Christopher Morris, Nils M. Kriege, Franka Bause, Kristian Kersting, Petra Mutzel, and Marion Neumann. Tudataset: A collection of benchmark datasets for learning with graphs. In *ICML 2020 Workshop on Graph Representation Learning and Beyond (GRL+ 2020)*, 2020.
- [55] Karsten M Borgwardt, Cheng Soon Ong, Stefan Schönauer, SVN Vishwanathan, Alex J Smola, and Hans-Peter Kriegel. Protein function prediction via graph kernels. *Bioinformatics*, 21(suppl_1):i47–i56, 2005.
- [56] Nikil Wale, Ian A Watson, and George Karypis. Comparison of descriptor spaces for chemical compound retrieval and classification. *Knowledge and Information Systems*, 14:347–375, 2008.
- [57] Christoph Helma, Ross D. King, Stefan Kramer, and Ashwin Srinivasan. The predictive toxicology challenge 2000–2001. *Bioinformatics*, 17(1):107–108, 2001.
- [58] Seongjun Yun, Minbyul Jeong, Raehyun Kim, Jaewoo Kang, and Hyunwoo J Kim. Graph transformer networks. *Advances in neural information processing systems*, 32, 2019.

- [59] Mengchun Zhang, Maryam Qamar, Taegoo Kang, Yuna Jung, Chen-shuang Zhang, Sung-Ho Bae, and Chaoning Zhang. A survey on graph diffusion models: Generative ai in science for molecule, protein and material. *arXiv preprint arXiv:2304.01565*, 2023.
- [60] Andrei Gabrielov and Nicolai Vorobjov. Complexity of stratification of semi-pfaffian sets. *Discrete & computational geometry*, 14(1):71–91, 1995.

A Proof of the main results

The proof of Theorems 1,3 and 4 adopts the same reasoning used in [41] and [3] to derive a bound on the VC dimension of feedforward neural networks and the original GNN model, respectively. Before proceeding with the proofs, let us introduce the required notation and some results from [41]. These results will provide us with the mathematical tools to represent the computation of GNNs with a set of Pfaffian equations and to bound the VC dimension based on the format of the functions involved in such equations.

A.1 Notation and results from the literature

Representing a set of equations by a logical formula

Formally, we use a theory in which a classifier is described by a logical formula that is constructed by combining Pfaffian equations. Thus, let τ_1, \dots, τ_s be a set of C^∞ (infinitely differentiable) functions from $\mathbb{R}^{\gamma+p}$ to \mathbb{R} . Suppose that $\Phi(\mathbf{y}, \boldsymbol{\theta})$, $\mathbf{y} \in \mathbb{R}^\gamma$, $\boldsymbol{\theta} \in \mathbb{R}^p$ is a quantifier-free logical formula constructed using the operators *and* and *or*, and atoms in the form of $\tau_i(\mathbf{y}, \boldsymbol{\theta}) = 0$. Note that, fixed $\boldsymbol{\theta}$, $\Phi(\cdot, \boldsymbol{\theta})$ takes as input a vector \mathbf{y} and returns a logical value, so that it can be considered as a classifier with input \mathbf{y} and parameters $\boldsymbol{\theta}$. Moreover, the formula can be also used to represent a set of Pfaffian equations, which corresponds to the case when Φ includes only the operator *and* and τ_i are Pfaffian. Actually, later, we will see that τ_1, \dots, τ_s can be specified so that Φ defines the computation of a GNN.

The VC dimension of Φ

The VC dimension of Φ can be defined in the usual way. Indeed, Φ is said to shatter a set $\mathcal{S} = \{\bar{\mathbf{y}}_1, \dots, \bar{\mathbf{y}}_r\}$ if, for any set of binary assignments $\boldsymbol{\delta} = [\delta_1, \dots, \delta_r] \in \{0, 1\}^r$, there exist parameters $\bar{\boldsymbol{\theta}}$ such that, for any i ,

$\Phi(\mathbf{y}_i, \bar{\boldsymbol{\theta}})$ is true if $\delta_i = 1$, and false if $\delta_i = 0$. Then, the VC dimension of Φ is defined as the size of the maximum set that Φ can shatter, i.e.,

$$\text{VCdim}(\Phi) = \max_{\mathcal{S} \text{ is shattered by } \Phi} |\mathcal{S}|.$$

Interestingly, the VC dimension of Φ can be bounded by studying the topological properties of the inverse image, in the parameter domain, of the functions τ_i [41]. More precisely, let $\bar{\mathbf{y}}_1, \dots, \bar{\mathbf{y}}_z$ be vectors in $\mathbb{R}^{\bar{\gamma}}$, and $\mathbf{T} : \mathbb{R}^{\bar{p}} \rightarrow \mathbb{R}^{\bar{u}}$, $\bar{u} \leq \bar{p}$, be defined as

$$\mathbf{T}(\bar{\boldsymbol{\theta}}) = [\bar{\tau}_1(\bar{\boldsymbol{\theta}}), \dots, \bar{\tau}_{\bar{u}}(\bar{\boldsymbol{\theta}})], \quad (7)$$

where $\bar{\tau}_1(\bar{\boldsymbol{\theta}}), \dots, \bar{\tau}_{\bar{u}}(\bar{\boldsymbol{\theta}})$ are functions of the form of $\tau_i(\bar{\mathbf{y}}_j, \bar{\boldsymbol{\theta}})$, i.e., for each r , $1 \leq r \leq \bar{u}$, there exist integers i and j such that $\bar{\tau}_r(\bar{\boldsymbol{\theta}}) = \tau_i(\bar{\mathbf{y}}_j, \bar{\boldsymbol{\theta}})$. Let $[\epsilon_1, \dots, \epsilon_{\bar{u}}]$ be a regular value ¹ of \mathbf{T} and assume that there exists a positive integer B that bounds the number of connected components of $\mathbf{T}^{-1}(\epsilon_1, \dots, \epsilon_{\bar{u}})$ and does not depend on the chosen $\epsilon_1, \dots, \epsilon_{\bar{u}}$ and on the selected $\bar{\mathbf{y}}_j$. Then, the following proposition holds [41].

Theorem 5. The VC dimension of Φ is bounded as follows:

$$\text{VCdim}(\Phi) \leq 2 \log B + \bar{p}(16 + 2 \log \bar{s}).$$

Therefore, Theorem 5 provides a bound on the VC dimension of Φ that depends on the number \bar{p} of parameters, the total number \bar{s} of functions τ_i , and the bound B on the number of connected components of \mathbf{T}^{-1} .

A bound on the number of connected components

A bound B on the number of connected components of \mathbf{T}^{-1} can be obtained based on known results from the literature. In particular, the following theorem provides a bound in the case of a set of Pfaffian equations.

Theorem 6 ([53]). Consider a system of equations $\bar{q}_1(\boldsymbol{\theta}) = 0, \dots, \bar{q}_k(\boldsymbol{\theta}) = 0$, where \bar{q}_i , $1 \leq i \leq k$, are Pfaffian functions in a domain $G \subseteq \mathbb{R}^{\bar{p}}$, having a common Pfaffian chain of length $\bar{\ell}$ and maximum degrees $(\bar{\alpha}, \bar{\beta})$. Then the number of connected components of the set $\{\boldsymbol{\theta} | \bar{q}_1(\boldsymbol{\theta}) = 0, \dots, \bar{q}_k(\boldsymbol{\theta}) = 0\}$ is bounded by

$$2^{\frac{\bar{\ell}(\bar{\ell}-1)}{2}+1}(\bar{\alpha} + 2\bar{\beta} - 1)^{\bar{p}-1}((2\bar{p}-1)(\bar{\alpha} + \bar{\beta}) - 2\bar{p} + 2)^{\bar{\ell}}.$$

¹We recall that $[\epsilon_1, \dots, \epsilon_{\bar{u}}]$ is a regular value of \mathbf{T} if either $\mathbf{T}^{-1}([\epsilon_1, \dots, \epsilon_{\bar{u}}]) = \emptyset$ or $\mathbf{T}^{-1}([\epsilon_1, \dots, \epsilon_{\bar{u}}])$ is a $(\bar{p} - \bar{u})$ -dimensional C^∞ -submanifold of $\mathbb{R}^{\bar{p}}$.

A.2 Proof of Theorem 1

First, we prove Theorem 1. The proofs of Theorems 3 and 4 will adopt the same argumentative scheme. As already mentioned, we will follow the reasoning in [41, 3], which consists of three steps. First, it is shown that the computation of GNNs can be represented by a set of equations defined by Pfaffian functions. Then, using the format of such Pfaffian functions, Theorem 6 allows to derive a bound on the number of connected components of the space defined by the equations. Finally, Theorem 5 provides a bound on the VC dimension of GNNs.

Let us define a set of equations $\tau_i(\mathbf{y}, \boldsymbol{\theta}) = 0$ that specifies the computation of the generic GNN model of Eq. (4). Here, $\boldsymbol{\theta}$ collects the GNN parameters, while \mathbf{y} contains all the variables necessary to define the GNN calculation, that is, some variables involved in the representation of the GNN input, i.e., the input graph, and other variables used for the representation of the internal features of the GNN.

More precisely, let us assume that $\text{COMBINE}^{(1)}$ has $p_{\text{comb}^{(1)}}$ parameters, $\text{COMBINE}^{(t)}$ has p_{comb} parameters for $2 \leq t \leq L$, $\text{AGGREGATE}^{(1)}$ has $p_{\text{agg}^{(1)}}$ parameters, $\text{AGGREGATE}^{(t)}$ has p_{agg} parameters for $2 \leq t \leq L$, and READOUT has p_{read} parameters.

Then, the dimension of $\boldsymbol{\theta}$ is $p_{\text{comb}^{(1)}} + p_{\text{agg}^{(1)}} + (L-1)(p_{\text{comb}} + p_{\text{agg}}) + p_{\text{read}}$. Moreover, for a given graph $\mathbf{G} = (G, \mathbf{L})$ in \mathcal{G} , \mathbf{y} contains some vectorial representation of \mathbf{G} , namely the Nq graph attributes in \mathbf{L}_G , and a vectorial representation of the adjacency matrix \mathbf{A} , which requires $N(N-1)/2$ elements. Besides, to define the equations, we use the same trick as in [41] and introduce new variables for each computation unit of the network. These variables belong to the input \mathbf{y} of τ . Formally, we consider a vector of d variables $\mathbf{h}_v^{(k)}$ for each node v and for each layer k . Note that, as we may be interested in defining multiple GNN computations on multiple graphs at the same time, here v implicitly addresses a specific node of some graph in the domain. Finally, a variable READOUT for each graph contains just a single output of the GNN. Thus, in total, the dimension of \mathbf{y} is $Nq + N(N-1)/2 + NdL + 1$.

Therefore, the computation of the GNN model in (4) is defined by the following set of $LNd + Nq + 1$ equations,

$$\mathbf{h}_v^{(0)} - \mathbf{L}_v = 0, \quad (8)$$

$$\mathbf{h}_v^{(t+1)} - \text{COMBINE}^{(t+1)}(\mathbf{h}_v^{(t)}, \text{AGGREGATE}^{(t+1)}(\{\mathbf{h}_u^{(t)} | u \in \text{ne}(v)\}, \mathbf{A})) = 0, \quad (9)$$

$$\overline{\text{READOUT}} - \text{READOUT}(\{\mathbf{h}_v^{(L)} : v \in V\}) = 0, \quad (10)$$

where \mathbf{A} is the variable storing the adjacency matrix of the input graph. We can assume that \mathbf{A} is valid for any finite graph.

The following lemma specifies the format of the Pfaffian functions involved in Eqs. (8)–(10).

Lemma 7. Let $\text{COMBINE}^{(t)}$, $\text{AGGREGATE}^{(t)}$ and READOUT be Pfaffian functions with format, respectively, $(\alpha_{\text{comb}}, \beta_{\text{comb}}, \ell_{\text{comb}})$, $(\alpha_{\text{agg}}, \beta_{\text{agg}}, \ell_{\text{agg}})$, $(\alpha_{\text{read}}, \beta_{\text{read}}, \ell_{\text{read}})$ w.r.t. the variables \mathbf{y} and $\boldsymbol{\theta}$ described above, then:

1. the left part of Eq. (8) is a polynomial of degree 1;
2. the left part of Eq. (9) is a Pfaffian function with format $(\alpha_{\text{agg}} + \beta_{\text{agg}} - 1 + \alpha_{\text{comb}}\beta_{\text{agg}}, \beta_{\text{comb}}, \ell_{\text{comb}} + \ell_{\text{agg}})$;
3. the left part of Eq. (10) is a Pfaffian function with format $(\alpha_{\text{read}}, \beta_{\text{read}}, \ell_{\text{read}})$;
4. Eqs. (8)–(10) constitute a system of Pfaffian equations with a maximal format $(\alpha_{\text{system}}, \beta_{\text{system}}, \ell_{\text{system}})$, where $\alpha_{\text{system}} = \max\{\alpha_{\text{agg}} + \beta_{\text{agg}} - 1 + \alpha_{\text{comb}}\beta_{\text{agg}}, \alpha_{\text{read}}\}$, $\beta_{\text{system}} = \max\{\beta_{\text{comb}}, \beta_{\text{read}}\}$ and $\ell_{\text{system}} = \text{LND}(\ell_{\text{comb}} + \ell_{\text{agg}}) + \ell_{\text{read}}$.

Proof. The first point is straightforwardly evident, while the third is true by definition. The second point can be derived by applying the composition lemma for Pfaffian functions [60], according to which, if two functions f and g have format $(\alpha_f, \beta_f, \ell_f)$ and $(\alpha_g, \beta_g, \ell_g)$, respectively, then their composition $f \circ g$ has format $(\alpha_g + \beta_g - 1 + \alpha_f\beta_g, \beta_f, \ell_f + \ell_g)$. Finally, the fourth point is obtained by taking the maximum of the format of the involved Pfaffian equations also observing that the common chain is the concatenation of the chains. \square

Now we can proceed with the proof of Theorem 1.

Proof. Let \mathbf{T} be defined as in Eq. (7), where $\tau_i(\mathbf{y}, \boldsymbol{\theta}) = 0$ are the equations in (8), (9), (10). Combining Theorem 6 with the formats provided by point 3. of Lemma 7, for any input graph and any value of the variables \mathbf{y} , the number of connected components of \mathbf{T}^{-1} satisfies

$$B \leq 2^{\frac{\bar{\ell}(\bar{\ell}-1)}{2}+1}(\bar{\alpha} + 2\bar{\beta} - 1)^{\bar{p}-1}((2\bar{p}-1)(\bar{\alpha} + \bar{\beta}) - 2\bar{p} + 2)^{\bar{\ell}}, \quad (11)$$

where $\bar{p} = p_{\text{comb}^{(1)}} + p_{\text{agg}^{(1)}} + (L-1)(p_{\text{comb}} + p_{\text{agg}}) + p_{\text{read}}$, $\bar{\alpha} = \alpha_{\text{system}}$, $\bar{\beta} = \beta_{\text{system}}$, $\bar{\ell} = \bar{p}(\text{LND}(\ell_{\text{comb}} + \ell_{\text{agg}}) + \ell_{\text{read}})$.

By Theorem 5, the VC dimension of the GNN described by Eqs. (8)–(10) is bounded by

$$\text{VCdim}(\text{GNN}) \leq 2 \log B + \bar{p}(16 + 2 \log \bar{s}), \quad (12)$$

where $\bar{s} = LNd + Nq + 1$. Thus, substituting Eq. (11) in Eq. (12), we have:

$$\begin{aligned} \text{VCdim}(\text{GNN}) &\leq 2 \log B + \bar{p}(16 + 2 \log \bar{s}) \\ &\leq 2 \log \left(2^{\frac{\bar{\ell}(\bar{\ell}-1)}{2}+1} (\bar{\alpha} + 2\bar{\beta} - 1)^{\bar{p}-1} ((2\bar{p}-1)(\bar{\alpha} + \bar{\beta}) - 2\bar{p} + 2)^{\bar{\ell}} \right) + \\ &\quad + \bar{p}(16 + 2 \log \bar{s}) \\ &= \bar{\ell}(\bar{\ell}-1) + 2(\bar{p}-1) \log(\bar{\alpha} + 2\bar{\beta} - 1) + 2\bar{\ell} \log((2\bar{p}-1)(\bar{\alpha} + \bar{\beta}) - 2\bar{p} + 2) + \\ &\quad + \bar{p}(16 + 2 \log \bar{s}) + 2, \end{aligned}$$

obtaining Eq. (5).

If we denote $H = LNd((\ell_{\text{comb}} + \ell_{\text{agg}}) + \ell_{\text{read}})$, we have:

$$\begin{aligned} \text{VCdim}(\text{GNN}) &\leq \bar{p}H(\bar{p}H - 1) + 2(\bar{p} - 1) \log(\alpha_{\text{system}} + 2\beta_{\text{system}} - 1) \\ &\quad + 2\bar{p}H \log((2\bar{p} - 1)(\alpha_{\text{system}} + \beta_{\text{system}}) - 2\bar{p} + 2) \\ &\quad + \bar{p}(16 + 2 \log(\bar{s})) + 2 \\ &\leq \bar{p}^2 H^2 + 2\bar{p} \log(3\gamma) \\ &\quad + 2\bar{p}H \log((4\gamma - 2)\bar{p} + 2 - 2\gamma) \\ &\quad + \bar{p}(16 + 2 \log(\bar{s})) + 2. \end{aligned} \quad (13)$$

Then, by replacing \bar{p} , H and \bar{s} , and setting $\gamma = \max\{\bar{\alpha}, \bar{\beta}\}$, it follows that:

$$\begin{aligned} \text{VCdim}(\text{GNN}) &\leq (p_{\text{comb}^{(1)}} + p_{\text{agg}^{(1)}} + (L-1)(p_{\text{comb}} + p_{\text{agg}}) + p_{\text{read}})^2 (LNd(\ell_{\text{comb}} + \ell_{\text{agg}}) + \ell_{\text{read}})^2 \\ &\quad + 2(p_{\text{comb}^{(1)}} + p_{\text{agg}^{(1)}} + (L-1)(p_{\text{comb}} + p_{\text{agg}}) + p_{\text{read}}) \log(3\gamma) \\ &\quad + 2(p_{\text{comb}^{(1)}} + p_{\text{agg}^{(1)}} + (L-1)(p_{\text{comb}} + p_{\text{agg}}) + p_{\text{read}}) \cdot \\ &\quad \cdot \log((4\gamma - 2)(p_{\text{comb}^{(1)}} + p_{\text{agg}^{(1)}} + (L-1)(p_{\text{comb}} + p_{\text{agg}}) + p_{\text{read}}) + 2 - 2\gamma) \\ &\quad + (p_{\text{comb}^{(1)}} + p_{\text{agg}^{(1)}} + (L-1)(p_{\text{comb}} + p_{\text{agg}}) + p_{\text{read}})(16 + 2 \log(LNd + Nq + 1)), \end{aligned}$$

which leads to Eq. (6) as in the thesis. \square

A.3 Proof of Theorem 2

The orders of growth of the VC dimension w.r.t. \bar{p}, N, L, d, q are straightforwardly derived by inspecting Eq. 6 in Theorem 1.

A.4 Proof of Theorem 3

As already mentioned in A.2, the proof of Theorem 3 follows the same scheme used in proof of Theorem 1. We just recall that we consider a GNN defined by the following updating equation:

$$\mathbf{h}_v^{(t+1)} = \sigma(\mathbf{W}_{\text{comb}}^{(t+1)} \mathbf{h}_v^{(t)} + \mathbf{W}_{\text{agg}}^{(t+1)} \mathbf{h}_{\text{ne}(v)}^{(t+1)} + \mathbf{b}^{(t+1)}), \quad (14)$$

where σ is the activation function and

$$\mathbf{h}_{\text{ne}(v)}^{(t+1)} = \sum_{u \in \text{ne}(v)} \mathbf{h}_u^{(t)}. \quad (15)$$

The hidden states are initialised as $\mathbf{h}_v^{(0)} = \mathbf{L}_v$. It is easily seen that the total number of parameters is $p = (2d + 1)(d(L - 1) + q + 1) - q$. Indeed, the parameters are:

- $\mathbf{W}_{\text{comb}}^{(1)}, \mathbf{W}_{\text{agg}}^{(1)} \in \mathbb{R}^{d \times q}, \mathbf{b}^{(1)} \in \mathbb{R}^{d \times 1}$, so that we have $2dq + d$ parameters;
- $\mathbf{W}_{\text{comb}}^{(t)}, \mathbf{W}_{\text{agg}}^{(t)} \in \mathbb{R}^{d \times d}, \mathbf{b}^{(t)} \in \mathbb{R}^{d \times 1}$ for $t = 2, \dots, L$, so that we have $(2d^2 + d)(L - 1)$ parameters;
- $\mathbf{w} \in \mathbb{R}^{1 \times d}, b \in \mathbb{R}$, so that we have $d + 1$ parameters.

Summing up, we will have $2dq + d + (2d^2 + d)(L - 1) + d + 1 = (2d + 1)(d(L - 1) + q + 1) - q$ parameters. By Eq. (14), the computation of the GNN is straightforwardly defined by the following set of $LNd + Nq + 1$ equations:

$$\mathbf{h}_v^{(0)} - \mathbf{L}_v = 0, \quad (16)$$

$$\mathbf{h}_v^{(t+1)} - \sigma\left(\mathbf{W}_{\text{comb}}^{(t+1)} \mathbf{h}_v^{(t)} + \sum_u \mathbf{W}_{\text{agg}}^{(t+1)} \mathbf{h}_u^{(t)} m_{v,u} + \mathbf{b}^{(t+1)}\right) = 0, \quad (17)$$

$$\text{READOUT} - \sigma\left(\sum_{v \in V} \mathbf{w} \mathbf{h}_v^{(L)} + b\right) = 0, \quad (18)$$

where $m_{v,u}$ is a binary value, which is 1 when v and u are connected and 0, otherwise.

Now we state the analogous of Lemma 7 to retrieve the format of Pfaffian functions involved in the above equations.

Lemma 8. Let σ be a Pfaffian function in \mathbf{x} with format $(\alpha_\sigma, \beta_\sigma, \ell_\sigma)$, then w.r.t. the variables \mathbf{y} and \mathbf{w} described above,

1. the left part of Eq. (16) is a polynomial of degree 1;
2. the left part of Eq. (17) is a Pfaffian function having format $(2 + 3\alpha_\sigma, \beta_\sigma, \ell_\sigma)$;

3. the left part of Eq. (18) is a Pfaffian function having format $(1 + 2\alpha_\sigma, \beta_\sigma, \ell_\sigma)$;
4. Eqs. (16)–(18) constitute a system of Pfaffian equations with format $(2 + 3\alpha_\sigma, \beta_\sigma, H\ell_\sigma)$, where the shared chain is obtained by concatenating the chains of $H = LNd + 1$ equations in (17), (18), including an activation function.

Proof. The first point is straightforwardly evident. The second and third points can be derived by applying the composition lemma for Pfaffian functions. Actually, the formula inside σ in Eq. (17) is a polynomial of degree 3, due to the factors $\mathbf{h}_u^{(t-1)} \mathbf{W}_{\text{agg}}^{(t)} m_{v,u}$, while the formula inside σ in Eq. (18) is a polynomial of degree 2, due to the factors $\mathbf{h}_v^{(L)} \mathbf{W}$. Moreover, polynomials are Pfaffian functions with null chains, α equals 0 and β equals their degrees. Thus, the functions inside σ in Eqs. (17) and (18) have format $(0, 3, 0)$ and $(0, 2, 0)$, respectively. Then, the thesis follows by the composition lemma [60], according to which if two functions f and g have format $(\alpha_f, \beta_f, \ell_f)$ and $(\alpha_g, \beta_g, \ell_g)$, respectively, then their composition $f \circ g$ has format $(\alpha_g + \beta_g - 1 + \alpha_f \beta_g, \beta_f, \ell_f + \ell_g)$. Finally, the fourth point is a consequence of the fact that the equations are independent and the chains can be concatenated. The length of the chain derives directly from the existence of $H = LNd + 1$ equations using σ . The degree is obtained copying the largest degree of a Pfaffian function, which is the one in Eq. (17). \square

As in A.2, it is enough to combine Lemma 8, Theorem 6 and Theorem 5 to obtain the bounds stated in the thesis. The bounds on the VC dimension of the specific GNN with `logsig` as activation function is easily found since the format of `logsig` is $(2, 1, 1)$:

$$\begin{aligned} \text{VCdim}(\text{GNN}) &\leq ((2d + 1)(d(L - 1) + q + 1) - q)^2 (LNd + 1)^2 \\ &\quad + 2((2d + 1)(d(L - 1) + q + 1) - q) \log(9) \\ &\quad + 2((2d + 1)(d(L - 1) + q + 1) - q) \log(16((2d + 1)(d(L - 1) + q + 1) - q)) \\ &\quad + ((2d + 1)(d(L - 1) + q + 1) - q)(16 + 2 \log(LNd + Nq + 1)). \end{aligned}$$

\square

Let us call Basic GNN (BGNN) the model of Eqs. (2)–(3). The proof is based on the introduction of an extended version, which we call EGNN, that can simulate the BGNN. Due to this capability, the EGNN can shatter any set that is shattered by the BGNN so that its VC dimension is greater or equal to the VC dimension of the BGNN. The proof will follow by bounding the VC dimension of the former model.

More precisely, the EGNN exploits the same aggregation mechanism of the BGNN to compute the features, which is described by Eq. (2). On the other hand, the **READOUT** function is defined as

$$\text{READOUT}\left(\{\mathbf{h}_v^{(L)} \mid v \in V\}\right) := f\left(\sum_{v \in V} \mathbf{w}\mathbf{h}_v^{(L)}c_v + b\right), \quad (19)$$

where c_v are additional real inputs used to weight each node feature in the **READOUT** function. The simulation is based on the following steps.

- 1) Each input graph G of the BGNN is transformed to another graph G' , where all the nodes having the same 1-WL color are merged into a single node and the edges are merged consequently;
- 2) The EGNN is applied to G' and each c_v is set equal to the number of nodes that have been merged to obtain node v .

Note that a GNN cannot distinguish nodes with the same color as the computation is the same on all these nodes. Thus, the BGNN and the EGNN produce the same features on nodes sharing color. As a consequence, also the **READOUTs** of the two models have the same output, when the c_v are equal to the number of nodes within each color cluster.

Given these assumptions, the number of equations describing the Pfaffian variety associated to the EGNN is reduced to $s_c = C_1d + C_0q + 1$, which can be used in place of \bar{s} in Theorem 5. Moreover, also the chains of the Pfaffian functions in merged equations can be merged and we have that H can be replaced by $H_c = C_1d + 1$. Finally, the length of the chain ℓ of Theorem 6 is replaced by $\bar{\ell}_c = \bar{p}H_c\ell_\sigma$.

With the above changes, we can replace the variables in Eq. (13) as in A.2, obtaining:

$$\begin{aligned} \text{VCdim(GNN)} &\leq \bar{p}H_c(\bar{p}H_c - 1) + 2\bar{p}\log(9) \\ &\quad + 2\bar{p}H_c\log(16\bar{p} - 7) \\ &\quad + \bar{p}(16 + 2\log(\bar{s}_c)) + 2 \\ &\leq \bar{p}^2(C_1d + 1)^2 + 2\bar{p}\log(9) \\ &\quad + 2\bar{p}(C_1d + 1)\log(16\bar{p} - 7) \\ &\quad + \bar{p}(16 + 2\log(C_1d + C_0q + 1)). \end{aligned}$$

and the thesis holds. □

B Experiments on other datasets

In this appendix, we report the additional results on the experiment E1, regarding the evolution of the difference between the training and the test set, for GNNs with activation function $f \in \{\text{arctan}, \tanh\}$, over a dataset $\mathcal{D} \in \{\text{PROTEINS}, \text{PTC-MR}\}$. Each figure shows the evolution of `diff` through the epochs, for certain values of `hd`, keeping fixed $l = 3$, and for certain values of l , keeping fixed `hd` = 32; for each figure, the picture on the left shows how `diff` evolves as the hidden size increases, while the picture on the right shows how `diff` evolves as the hidden size, or the number of layers, increases.

The experiments reported here confirm the same conclusion drawn in Section 5.

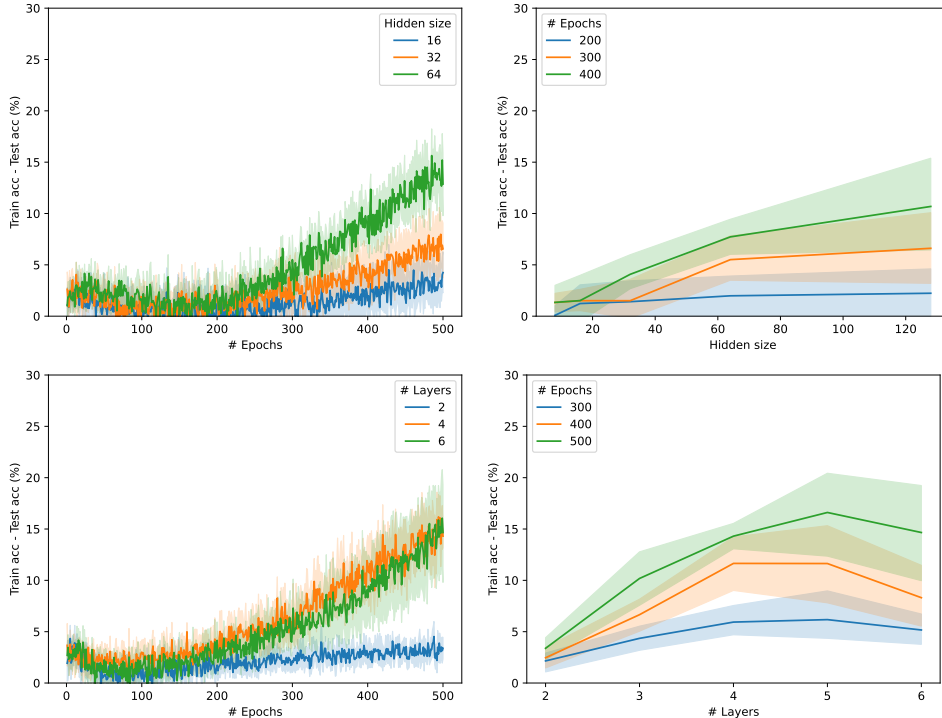


Figure 4: Results on the task **E1** for GNNs with activation function atan over the dataset **PROTEINS**.

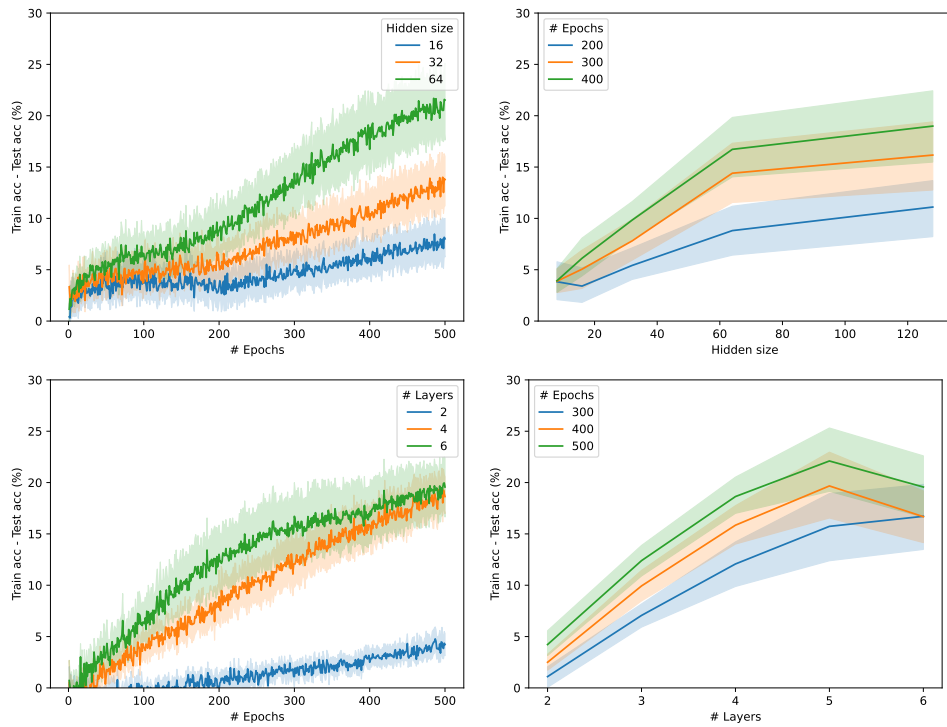


Figure 5: Results on the task **E1** for GNNs with activation function atan over the dataset **PTC-MR**.

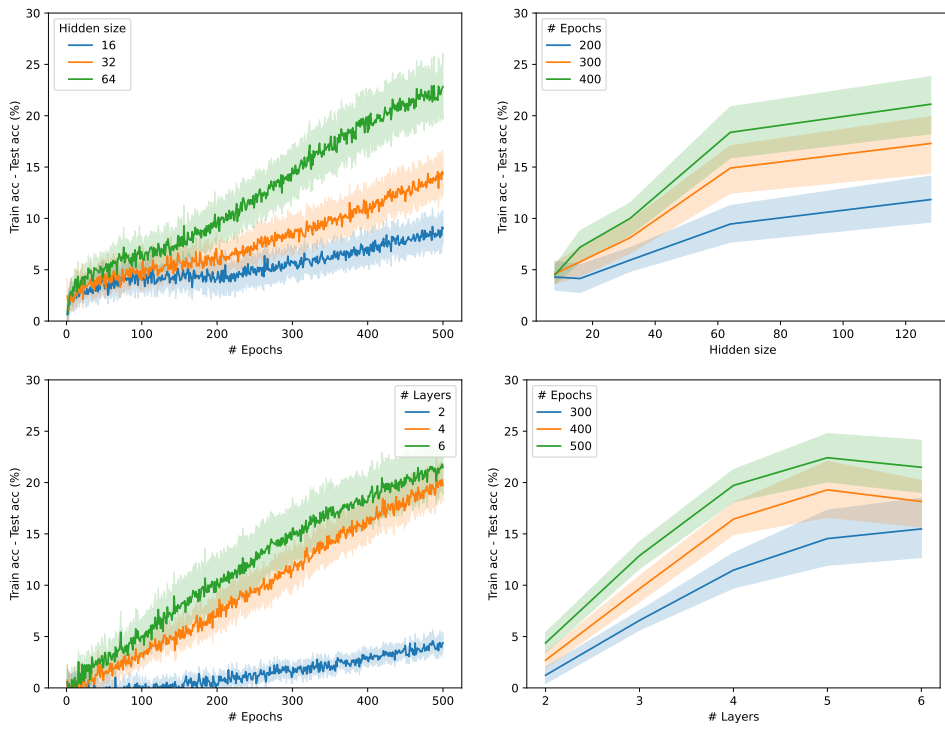


Figure 6: Results on the task **E1** for GNNs with activation function `tanh` over the dataset **PROTEINS**.

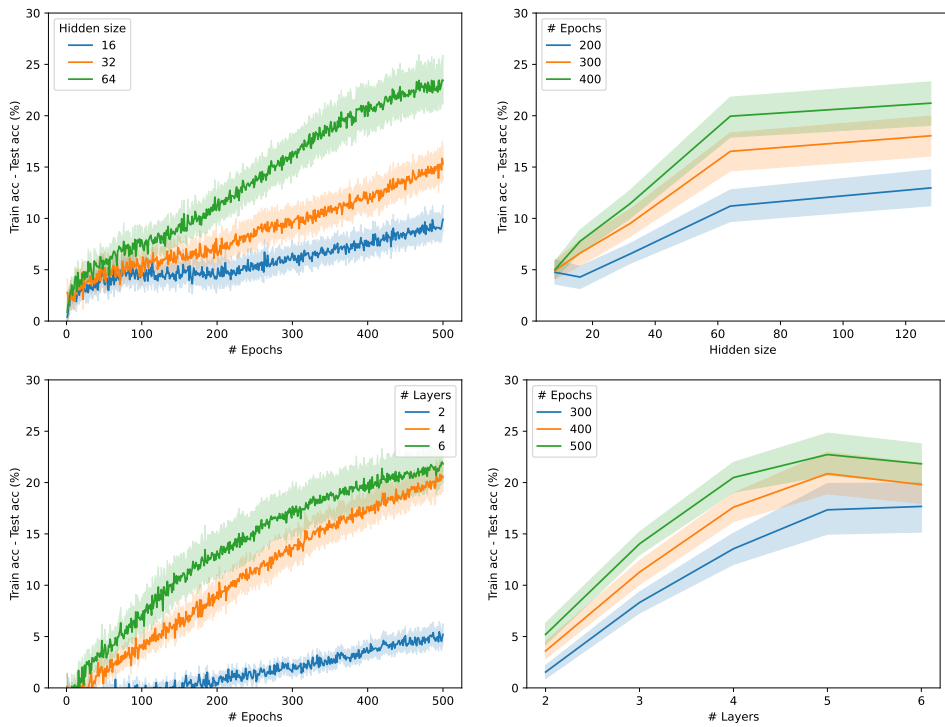


Figure 7: Results on the task **E1** for GNNs with activation function `tanh` over the dataset **PTC-MR**.